

## SYNTHESIS AND PROPERTIES OF INORGANIC COMPOUNDS

# Hydrogenation of Intermetallic Compound $\text{Mg}_{17}\text{Al}_{12}$

V. N. Fokin<sup>a, \*</sup>, P. V. Fursikov<sup>a</sup>, E. E. Fokina<sup>a</sup>,  
I. I. Korobov<sup>a</sup>, A. M. Fattakhova<sup>a, b</sup>, and B. P. Tarasov<sup>a</sup>

<sup>a</sup>*Institute of Problems of Chemical Physics, Russian Academy of Sciences,  
Chernogolovka, Moscow oblast, 142432 Russia*

<sup>b</sup>*Moscow State University, Moscow, 119991 Russia*

\*e-mail: fvn@icp.ac.ru

Received January 25, 2019; revised February 26, 2019; accepted April 15, 2019

**Abstract**—A 200-micron powder of  $\gamma\text{-Mg}_{17}\text{Al}_{12}$  was reacted with hydrogen and ammonia at temperatures in the range 20–500°C with the goal to determine optimal hydrogenation parameters for this intermetallic compound as a potential hydrogen storage material. Direct hydriding of the intermetallic compound was found to occur at 390°C, but was accompanied by decomposition to a mixture of magnesium hydride with aluminum containing 4 wt % hydrogen. The hydriding of the intermetallic compound by ammonia was also accompanied by the appearance of magnesium hydride in the reaction product, but at 300°C. The hydrogen capacity of the products of reaction between the intermetallic compound and ammonia at 350°C was 3.9 wt % hydrogen. The product of ammonia treatment of the intermetallic compound  $\text{Mg}_{17}\text{Al}_{12}$  at 450–500°C was a mixture of aluminum with magnesium nitride.

**Keywords:** hydrogen, ammonia, intermetallic compound, hydrogenation, phase transformations

**DOI:** 10.1134/S0036023619090122

## INTRODUCTION

The role of magnesium and its compounds and alloys among the metals and polymetallic phases as promising materials for hydrogen storage in metal hydride accumulators is widely known [1–4]. Along with the advantages, however, there are serious problems in the practical use of magnesium for hydrogen storage, namely, high temperature of hydrogenation and dehydrogenation reactions in the  $\text{Mg-H}_2$  system, a high heat of reaction, and a slow rate of hydrogenation.

## THEORY

Various strategies and methods exist for facilitating hydrogenation [5–8]. One efficient method is to alloy magnesium with 4–10 at % aluminum [5, 9–12]. The effect of aluminum to increase the magnesium hydrogenation rate is due to the presence of the intermetallic compound  $\text{Mg}_{17}\text{Al}_{12}$  on the magnesium surface [5] or at grain interfaces [9], the formation of supersaturated  $\text{Mg}(\text{Al})$  solid solutions [10], microstructural modification of  $\text{Mg-Al}$  alloys, and phase transformations [11].

Nearly in all publications the authors mention that aluminum increases the magnesium hydrogenation rate due to the formation of the intermetallic compound  $\text{Mg}_{17}\text{Al}_{12}$  (what is called the  $\gamma$ -phase) and its hydride. When an  $\text{Mg} + 10$  at %  $\text{Al}$  powder mixture is

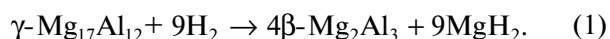
heated at 420°C, for example, aluminum is alloyed with magnesium to form, on the surface of magnesium particles, the intermetallic compound  $\text{Mg}_{17}\text{Al}_{12}$  that is free of the oxide and reacts with hydrogen at 340°C. The hydrogen evolved from the nascent hydride phase reacts with magnesium particles [5]. In addition, the formation of  $\text{Mg}_{17}\text{Al}_{12}$  was observed when the hydrogen-sorbing properties of the  $\text{MgH}_2\text{-AlH}_3$  (2 : 1) composite system were studied [13]. The  $\text{MgH}_2\text{-}10$  wt % composite  $\text{Mg}_{17}\text{Al}_{12}$  produced in a ball mill from the intermetallic compound and magnesium hydride, showed higher hydrogen absorption rates and higher hydrogen capacity compared to  $\text{MgH}_2$  [14]. The hydrogen capacity of the composite increased as the hydriding temperature increased, from 1.12 wt % at 120°C to 6.50 wt % at 200°C; this trend was assigned to the synergistic effect of the catalytic activity of the intermetallic compound and the defects that appeared on the magnesium surface in the course of composite production [14].

The intermetallic compound  $\gamma\text{-Mg}_{17}\text{Al}_{12}$  formed in the  $\text{Al-Mg}$  system melts congruently at 470°C, is isostructural to  $\alpha\text{-Mn}$ , and crystallizes in cubic crystal system with the unit cell parameter  $a = 10.4691\text{--}10.5916$  Å [15]. The range of values for the unit cell parameters is due to the intermetallic compound having a homogeneity range of 55–62.5 at %  $\text{Mg}$  (theoretically, the  $\gamma$ -phase of composition  $\text{Mg}_{17}\text{Al}_{12}$  contains 58.62 at % magnesium) [16].

The hydrogen-sorbing properties of the intermetallic compound were noted to depend on the preparation method [17]: the highest hydrogen capacity (4 wt %) was found in the hydride phase of an alloy prepared by sintering, rapidly quenched, and then treated in a ball mill and hydrided at 320°C. The alloys prepared using a ball mill have nanometer particle sizes.

The  $p$ - $c$  isotherms at 250°C in the  $\text{Mg}_{17}\text{Al}_{12}$ - $\text{H}_2$  system feature a plateau corresponding to hydride formation at 0.06 MPa (upon desorption, 0.04 MPa), and this proves the ability of the alloy to absorb 3.2 wt % hydrogen under 5.3 MPa and desorb it at 250°C [18].

When hydrided at 300°C [15, 16], the intermetallic compound decomposes to yield the hydride  $\text{MgH}_2$  and the intermetallic compound  $\beta$ - $\text{Mg}_2\text{Al}_3$ , the latter not reacting with hydrogen at this temperature:



When the temperature rises further to 350°C under a hydrogen atmosphere, the newly formed intermetallic compound  $\beta$ - $\text{Mg}_2\text{Al}_3$  decomposes by the reaction



Thus, a mixture of aluminum (or the aluminum-base solid solution  $\text{Mg}_{0.1}\text{Al}_{0.9}$  as reported earlier [19]) with magnesium hydride is the final product of hydriding  $\gamma$ - $\text{Mg}_{17}\text{Al}_{12}$  in the temperature range 250–350°C [18, 20]; this fact makes the intermetallic compound unsuitable for use in hydrogen accumulators. One solution to this problem is to reduce the hydriding temperature, i.e., to elucidate milder synthetic conditions for the hydride phase. We showed [21–23] that, in some cases, ammonia used, instead of hydrogen, for hydrogenation of metals, alloys, and intermetallic compounds provides milder conditions for the formation of hydride phases with the initial metal lattice being conserved.

The goal of this study was to determine the conditions for hydriding the intermetallic compound  $\gamma$ - $\text{Mg}_{17}\text{Al}_{12}$  with hydrogen and ammonia without hydrogenolysis and disproportionation.

## SUBJECTS AND METHODS

Intermetallic compound  $\text{Mg}_{17}\text{Al}_{12}$  samples were prepared by alloying the batch of constituent metals, which were 99.95% (Mg) and 99.99% (Al) pure, in an electric arc furnace with a non-consumable tungsten electrode under a pressure of purified argon (0.2 MPa).

An X-ray powder diffraction analysis of the samples was carried out on an ADP-1 diffractometer ( $\text{CuK}_\alpha$ -radiation). The error in unit cell parameters did not exceed 0.005 Å. The Le Bail full-profile refinement was performed in software PowderCell 3.3.

The microstructure and local elemental composition of the alloy were studied by scanning electron microscopy (SEM) in secondary and back-scattered electrons and energy-dispersive X-ray analysis (EDX)

using a VEGA TESCAN electron microscope at the accelerating voltage 20 kV. A polished section was prepared by grinding an alloy sample on abrasive cloths followed by final polishing with a 1- $\mu\text{m}$  diamond suspension.

The thermal stability of reaction products was studied on a STA 409 Luxx (Netzsch) simultaneous TG-DTA/DSC thermal analyzer. Weight loss (TG) curves and differential scanning calorimetry (DSC) curves were recorded under programmed heating at 10 deg/min in flowing argon.

The specific surface areas  $S_{\text{sp}}$  of samples were determined as the low-temperature krypton adsorption after volatiles were removed from the solid phase in a vacuum of  $1.3 \times 10^{-3}$  Pa at 300°C for 5 h and calculated by the Brunauer-Emmett-Teller method. The determination error was  $\pm 10\%$ .

The compositions of the produced phases were determined by volumetric and chemical analyses. The hydrogen and nitrogen were determined on a Vario Micro cube Elementar CHNS/O analyzer. The chlorine was determined turbidimetrically.

The hydrogen pressure was measured on an MO reference gage, Class 0.4.

## EXPERIMENTAL

Alloy powders to be treated with hydrogen and ammonia were prepared by grinding beads in a metal mortar followed by screening the 200  $\mu\text{m}$  particle size fraction. The specific surface area  $S_{\text{sp}}$  of these powders was 0.08  $\text{m}^2/\text{g}$ .

The intermetallic compound was hydrided by high-purity hydrogen (99.99%), which was evolved under heating by a metal hydride accumulator based on the intermetallic compound  $\text{LaNi}_5$ .

Ammonium chloride (chemically pure grade) was dried under vacuo for 9 h at 150°C. The  $\text{NH}_3$  dried over metallic sodium was 99.99% pure.

The alloy powder was hydrided by hydrogen or ammonia in a stainless steel container placed in the autoclave reactor of a 60-mL laboratory high-pressure setup.

Before being hydrided by hydrogen, an alloy sample 2–3 g in size was degassed in vacuo ( $\sim 1$  Pa) at room temperature or at 300–450°C for 1 h, and at the same temperature the autoclave was filled with hydrogen under 3.0–4.5 MPa. After the hydriding was over, the autoclave with the sample was kept for several hours at room temperature to attain equilibrium.

The reactions of alloy powders with ammonia were studied at the initial ammonia pressure 0.6–0.8 MPa using  $\text{NH}_4\text{Cl}$  (10 wt % of the amount of the intermetallic compound) as the process activator in a stainless steel container placed in the autoclave reactor of a 60-mL laboratory high-pressure setup. A weight of the prepared powder mixture (0.8–1.0 g) was evacuated to the

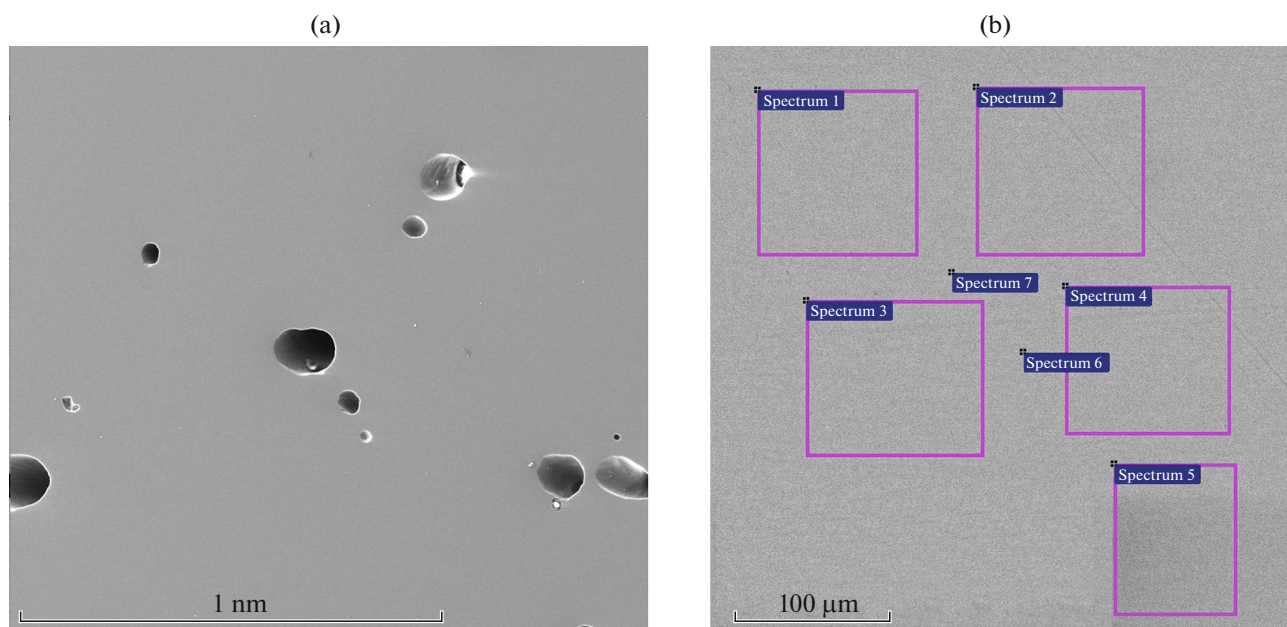


**Fig. 1.** (a) Secondary electron and (b) back-scattered electron micrographs of areas in a polished section of the alloy.

pressure  $\sim 0.13$  Pa for 30 min at room temperature, then ammonia was fed to the reactor, and the reactor was left to stand for 30 min. Then, the reactor was heated to the set temperature, exposed for 3 h, cooled to  $\sim 20^\circ\text{C}$ , and then again heated. Since the pressure in the system increased in the course of the reaction (to 1.5 MPa), the end of the process was judged from the cessation of change in pressure. After several heating–cooling cycles, ammonia was released to a buffer capacity, the reaction products were discharged under an inert atmosphere and then analyzed.

The  $\text{NH}_4\text{Cl}$  was removed from the reaction products by absolute ethanol under stirring for 1 h at room temperature (this procedure was repeated twice).

## RESULTS AND DISCUSSION

The alloy was a single phase according to X-ray powder diffraction and chemical analysis. SEM micrographs (Fig. 1) and EDX data obtained from various areas (Table 1), which coincide with one another to the error bar, imply that an alloy sample

has a homogeneous microstructure and a homogeneous elemental composition.

The X-ray powder diffraction pattern of the alloy (Fig. 2) features only reflections corresponding to the intermetallic compound  $\text{Mg}_{17}\text{Al}_{12}$  phase (the  $\gamma$ -phase in the Mg–Al phase diagram [15]) whose unit cell parameter is  $a = 10.5196$  Å; this value falls within the parameter  $a$  range established due to the homogeneity range.

The alloy was degassed at room temperature in vacuo ( $\sim 1$  Pa) for 1 h, then it was hydrided for 1.5 months at the initial hydrogen pressure 3.0 MPa also at room temperature. The thus-prepared product contained 0.1 wt % hydrogen as determined by chemical analysis; that is, hydriding produces a hydrogen solid solution in the intermetallic compound with the unit cell parameter  $a = 10.5205$  Å (Fig. 3). The specific surface area of the product is  $0.33$  m<sup>2</sup>/g, which also argues for the changes experienced by the sample in the course of hydriding. As probed by DTA, heating of the hydrogenation product is accompanied with a gradual weight loss

**Table 1.** EDX (wt %) data obtained at two sites and over five areas sized  $\sim 100 \times 100$  μm each (the magnesium content in stoichiometric  $\text{Mg}_{17}\text{Al}_{12}$  is 56.07 wt %)

| Metal | At a site      |                | Over an area   |                |                |                 |                |
|-------|----------------|----------------|----------------|----------------|----------------|-----------------|----------------|
|       | 6              | 7              | 1              | 2              | 3              | 4               | 5              |
| Mg    | $52.9 \pm 0.7$ | $52.7 \pm 0.8$ | $52.9 \pm 0.7$ | $52.5 \pm 0.7$ | $52.5 \pm 0.7$ | $52.85 \pm 0.7$ | $52.8 \pm 0.7$ |
| Al    | $47.1 \pm 1.1$ | $47.3 \pm 1.1$ | $47.1 \pm 1.1$ | $47.5 \pm 1.1$ | $47.5 \pm 1.1$ | $47.15 \pm 1.1$ | $47.2 \pm 1.1$ |

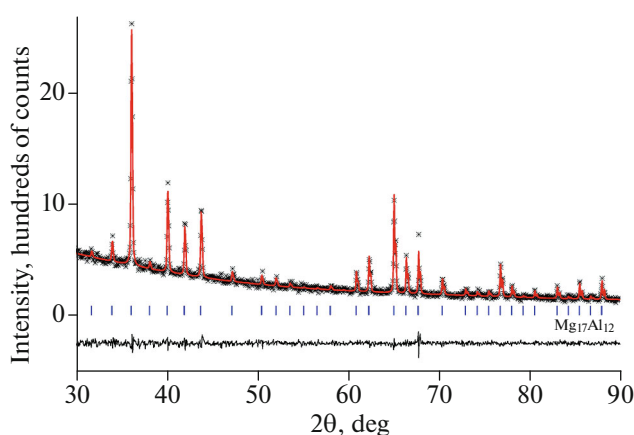


**Fig. 2.** X-ray powder diffraction pattern of the alloy and a calculated diffraction pattern of a crystalline bcc phase, space group  $I443m$  (no. 217), that corresponds to the  $Mg_{17}Al_{12}$  phase of  $\alpha$ -Mn type structure (solid curve). Vertical bars indicate the Bragg reflection positions from this phase whose relative intensities are at least 0.5%. The difference spectrum is shown below.

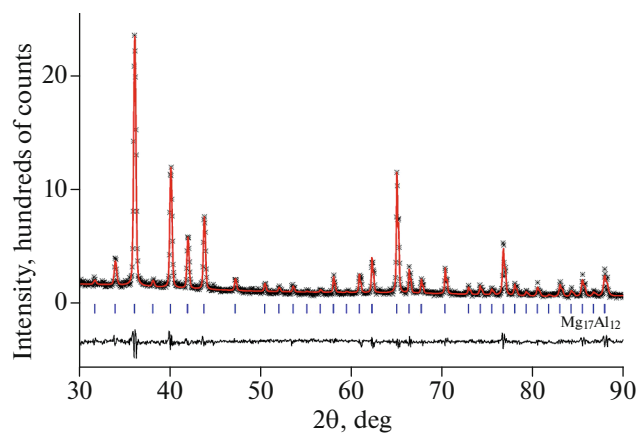


**Fig. 3.** X-ray powder diffraction pattern of the alloy after it was hydrided for 1.5 months at an initial hydrogen pressure of 3.0 MPa. The solid curve is the calculated X-ray diffraction pattern of a crystalline bcc phase, space group  $I443m$  (no. 217), that corresponds to the  $Mg_{17}Al_{12}$  phase of  $\alpha$ -Mn type structure. Vertical bars indicate the Bragg reflection positions from this phase whose relative intensities are at least 0.5%. The difference spectrum is shown below.

until an endothermic peak appears at  $\sim 470^\circ\text{C}$ , corresponding to the  $Mg_{17}Al_{12}$  melting temperature.

A rise of the degassing temperature (1 h) and the hydriding temperature (45 h, 30 cycles of 1.5 h each) to  $300^\circ\text{C}$  under the hydrogen pressure 4.0 MPa does not give rise to alloy hydriding; that is, the alloy does not decompose by Eq. (1) under these conditions, likely, due to the initial powder being coarse-grained.

When the intermetallic compound is hydrided at  $350^\circ\text{C}$  after being degassed at the same temperature (1 h) and at the hydrogen pressure 3.0 MPa with the overall synthesis time of 24 h, the intermetallic compound partially decomposes to yield magnesium hydride  $\alpha$ - $MgH_2$  ( $a = 4.5182 \text{ \AA}$ ,  $c = 3.0188 \text{ \AA}$ ) and trace aluminum, as probed by X-ray powder diffraction. It is only when the hydriding temperature rises to  $390^\circ\text{C}$  that the alloy decomposes completely to yield a mixture of magnesium hydride and aluminum, where the hydrogen content in the mixture does not exceed 4 wt %.

The product of hydrogen treatment of the alloy at  $450^\circ\text{C}$ , after being degassed, was identified by chemical analysis and X-ray powder diffraction as the initial intermetallic compound ( $a = 10.5258 \text{ \AA}$ ) with an admixture of trace aluminum. The formation of the initial intermetallic compound argues for the recombination of decomposition products and proves this well-documented fact [13, 16].

The conditions and results of ammonia treatment of the intermetallic compound are listed in Table 2. The heating time in each synthesis was 30 h. From the compositions of reaction products, one can see the strong and decisive effect of temperature on the reaction route.

Ammoniac treatment at  $100^\circ\text{C}$  (Table 2, sample 1) also yields a hydrogen solid solution in the intermetallic compound ( $a = 10.5262 \text{ \AA}$ ) with a simultaneous micronization of the alloy and a considerable (by several orders of magnitude) increase in its specific surface area (from 0.08 to  $10.0 \text{ m}^2/\text{g}$ ).

A rise in reaction temperature to  $150^\circ\text{C}$  (Table 2, sample 2) causes a slow decomposition of the initial intermetallic compound, as evidenced by the appearance of traces of magnesium amide  $Mg(NH_2)_2$  in the reaction products. The amount of the amide considerably increases as the reaction temperature rises further to  $200^\circ\text{C}$  (for  $Mg(NH_2)_2$  the unit cell parameters are  $a = 10.37 \text{ \AA}$ ,  $c = 20.15 \text{ \AA}$ ; Table 2, sample 3), but upon treatment at  $250^\circ\text{C}$  (Table 2, sample 4), this amount again decays to traces due to the decomposition of the amide.

Ammoniac treatment at  $150$ – $200^\circ\text{C}$  (Table 2, samples 2 and 3) also yields a hydrogen solid solution in the intermetallic compound  $Mg_{17}Al_{12}H_x$ . A rise in temperature to  $250^\circ\text{C}$  (Table 2, sample 4) causes a more complete hydriding of the intermetallic compound to yield a hydride phase with the parameter  $a = 10.5571 \text{ \AA}$ .

Figure 4 shows thermoanalytical curves for the reaction products of the intermetallic compound with ammonia at  $200^\circ\text{C}$  (Table 2, sample 3). The DSC curve features four endothermic peaks at 113, 189, 304, and  $470^\circ\text{C}$ , the temperatures at which adsorbed ammonia is evolved, magnesium amide decomposes, ammonium chloride decomposes, and the intermetallic compound melts, respectively.

The ammoniac treatment of the alloy at  $300^\circ\text{C}$  (Table 2, sample 5) is accompanied with the formation

**Table 2.** Parameters and results of a reaction between ammonia and intermetallic compound Mg<sub>17</sub>Al<sub>12</sub>

| Sample no. | Synthesis parameters |  | Reaction products  |                            |                  |  |
|------------|----------------------|--|--|----------------------------|------------------|--|
|            | <i>T</i> , °C        | <i>p</i> <sub>NH<sub>3</sub></sub> , MPa | phase composition  | unit cell parameters, Å    |                  | <i>S</i> <sub>sp</sub> , m <sup>2</sup> /g |
|            |                      |  |  | <i>a</i>                   | <i>c</i>         |  |
| 1          | 100                  | 0.84                                     | Mg <sub>17</sub> Al <sub>12</sub> H <sub><i>x</i></sub>  | 10.5262                    | —                | 10.0                                       |
| 2          | 150                  | 0.86                                     | Mg <sub>17</sub> Al <sub>12</sub> H <sub><i>x</i></sub><br>Mg(NH <sub>2</sub> ) <sub>2</sub> * | 10.5214                    | —                | 13.9                                       |
| 3          | 200                  | 0.86                                     | Mg <sub>17</sub> Al <sub>12</sub> H <sub><i>x</i></sub><br>Mg(NH <sub>2</sub> ) <sub>2</sub>   | 10.5256<br>10.37           | —<br>20.15       | 16.2                                       |
| 4          | 250                  | 0.86                                     | Mg <sub>17</sub> Al <sub>12</sub> H <sub><i>x</i></sub><br>Mg(NH <sub>2</sub> ) <sub>2</sub> * | 10.5571                    | —                | 15.6                                       |
| 5          | 300                  | 0.84                                     | Mg <sub>17</sub> Al <sub>12</sub> H <sub><i>x</i></sub><br>α-MgH <sub>2</sub>                  | 10.5755<br>4.5069          | —<br>3.0161      | 14.7                                       |
| 6          | 350                  | 0.77                                     | α-MgH <sub>2</sub><br>Mg <sub>2</sub> Al <sub>3</sub><br>Al                                    | 4.5030<br>28.220<br>4.0515 | 3.0210<br>—<br>— | 4.5  |
| 7          | 400                  | 0.77                                     | α-MgH <sub>2</sub><br>Mg <sub>2</sub> Al <sub>3</sub><br>Al                                    | 4.5100<br>28.230<br>4.0529 | 3.0190<br>—<br>— | 8.0  |
| 8          | 450                  | 0.74                                     | Al<br>Mg <sub>3</sub> N <sub>2</sub>   | 4.0531<br>9.9595           | —<br>—           | 6.3  |
| 9          | 500                  | 0.79                                     | Al<br>Mg <sub>3</sub> N <sub>2</sub>   | 4.0528<br>9.9635           | —<br>—           | 11.5                                       |

\*Traces.

of magnesium hydride α-MgH<sub>2</sub> (*a* = 4.5069 Å, *c* = 3.0161 Å), with the hydride phase Mg<sub>17</sub>Al<sub>12</sub>H<sub>*x*</sub> being conserved as the second reaction product. As the temperature rises further to 350°C (Table 2, sample 6), the reaction with ammonia follows Eq. (2) with the complete disappearance of the intermetallic hydride phase from the reaction products, the appearance of products of its decomposition (the intermetallic compound Mg<sub>2</sub>Al<sub>3</sub> and aluminum, *a* = 28.220 and 4.0515 Å, respectively), and the conservation of the magnesium dihydrides phase. The hydrogen amount in the reaction products obtained at 300 and 350°C (Table 2, samples 5 and 6) does not exceed 4.1 wt %. The product composition obtained for sample 6 (Table 2) is conserved when the reaction is carried out at 400°C (Table 2, sample 7).

The product of the ammoniac treatment of Mg<sub>17</sub>Al<sub>12</sub> at 450–500°C (Table 2, samples 8 and 9) is a mixture of aluminum with magnesium nitride, the

latter being produced by magnesium hydride decomposition.

Noteworthy are a great differentiation in the specific surface areas of the products (see Table 2) and the absence of any regular trend in these values; a likely reason for these observations is the different reaction routes with ammonia at different temperatures, and, accordingly, the different particle sizes of the materials formed. In addition, some contribution into the decrease in specific surface areas comes from sintering of the powder mixture at higher temperatures.

## CONCLUSIONS

The hydrogenation of a 200-μm powder of the intermetallic compound Mg<sub>17</sub>Al<sub>12</sub> by hydrogen occurs at 390°C and yields a mixture of magnesium hydride with aluminum; the hydrogen in the reaction product amounts to no more than 4 wt %. Likely, the coarse grain size of the intermetallic compound powder

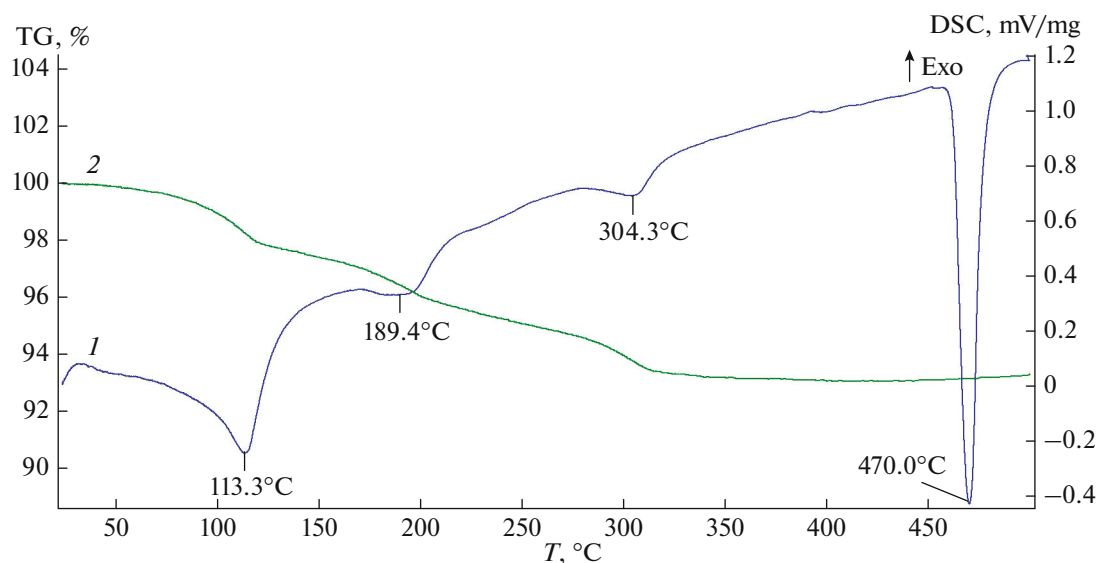


Fig. 4. Thermoanalytical curves for sample 3: (1) DSC and (2) TG curves.

inhibits the happening of the above-described two-stage hydriding scheme and makes it impossible to use mild synthesis to prepare a product with the maximal amount of hydrogen. In its turn, ammoniac hydrogenation of the intermetallic compound is accompanied with the appearance of magnesium hydride in the products, but at 300°C, which is 50°C lower than the reaction temperature for hydriding by hydrogen. The hydrogen capacity of the products of reacting the intermetallic compound with ammonia at 350°C is 3.9 wt % hydrogen, and the presence of the intermetallic compound  $Mg_2Al_3$  in the products argues for the two-stage character of the process. The inference about the effect caused by the powder particle size on the route and results of hydriding gives us grounds to continue attempts at optimizing the conditions for hydriding alloys in the Mg–Al system to decrease the grain size of the intermetallic compound, and this can be achieved in eutectic alloys and alloys modified by plastic strain as subject matters.

#### FUNDING

This study was supported by the Ministry of Education and Science of Russia (agreement no. 05.574.21.0209; unique identifier RFMEFI57418X0209).

#### REFERENCES

1. B. P. Tarasov, M. V. Lototskii, V. A. Yartys', Russ. J. Gen. Chem. **77**, 694 (2007).  
<https://doi.org/10.1134/S1070363207040429>
2. B. P. Tarasov, A. A. Arbutov, S. A. Mozhzhukhin, et al., Russ. J. Struct. Chem. **59**, 830 (2018).  
<https://doi.org/10.1134/S0022476618040121>
3. V. N. Fokin, E. E. Fokina, S. A. Mozhzhukhin, et al., Altern. En. Ekol., Nos. 9–10, 58 (2016).  
<https://doi.org/10.15518/isjaee.2016.09-010.058-065>
4. P. V. Fursikov and B. P. Tarasov, Russ. Chem. Bull. **67**, 193 (2018).  
<https://doi.org/10.1007/s11172-018-2058-y>
5. Y. Zhu, S. Luo, H. Lin, et al., J. Alloys Compd. **712**, 44 (2017).  
<https://doi.org/10.1016/j.jallcom.2017.04.049>
6. H. Yu, S. Bennici, and A. Auroux, Int. J. Hydrogen En. **39**, 11633 (2014).  
<https://doi.org/10.1016/j.ijhydene.2014.05.069>
7. R. R. Shahi, A. Bhataganar, S. K. Pandey, et al., Int. J. Hydrogen En. **40**, 11506 (2015).  
<https://doi.org/10.1016/j.ijhydene.2015.03.162>
8. V. N. Fokin, E. E. Fokina, and B. P. Tarasov, Russ. J. Inorg. Chem. **63**, 1605 (2018).  
<https://doi.org/10.1134/S0036023618120082>
9. M. Azizieh, M. Mazaheri, Z. Balak, et al., Mater. Sci. Eng. A **712**, 655 (2018).  
<https://doi.org/10.1016/j.msea.2017.12.030>
10. H. C. Zhong, H. Wang, and L. Z. Ouyang, Int. J. Hydrogen En. **39**, 3320 (2014).  
<https://doi.org/10.1016/j.ijhydene.2013.12.074>
11. M. Tanniru, D. K. Slattery, and F. Ebrahimi, Int. J. Hydrogen En. **36**, 639 (2011).  
<https://doi.org/10.1016/j.ijhydene.2010.09.083>
12. M. Tanniru, D. K. Slattery, and F. Ebrahimi, Int. J. Hydrogen En. **35**, 3555 (2010).  
<https://doi.org/10.1016/j.ijhydene.2010.03.109>
13. M. Ismail, Mater. Today: Proc. **3S**, 80 (2016).  
<https://doi.org/10.1016/j.matpr.2016.01.011>
14. X. L. Wang, J. P. Tu, P. L. Zhang, et al., Int. J. Hydrogen En. **32**, 3406 (2007).  
<https://doi.org/10.1016/j.ijhydene.2007.03.003>

15. *Phase Diagrams of Binary Metal Systems: A Handbook*, Ed. by N. P. Lyakishev (Mashinostroenie, Moscow, 1996), Vol. 1 [in Russian].
16. J.-C. Crivello, T. Nobuki, and T. Kuji, *Intermetallics* **15**, 1432 (2007).  
<https://doi.org/10.1016/j.intermet.2007.05.001>
17. W. Peng, Z. Lan, W. Wei, et al., *Int. J. Hydrogen En.* **41**, 1759 (2016).  
<https://doi.org/10.1016/j.ijhydene.2015.11.138>
18. H. Yabe and T. Kuji, *J. Alloys Compd.* **433**, 241 (2007).  
<https://doi.org/10.1016/j.jallcom.2006.06.043>
19. Q. A. Zhang and H. Y. Wu, *Mater. Chem. Phys.* **94**, 69 (2005).  
<https://doi.org/10.1016/j.matchemphys.2005.04.013>
20. J.-C. Crivello, T. Nobuki, S. Kato, et al., *J. Alloys Compd.* **446–447**, 157 (2007).  
<https://doi.org/10.1016/j.jallcom.2006.12.055>
21. V. N. Fokin, E. E. Fokina, I. I. Korobov, et al., *Russ. J. Inorg. Chem.* **59**, 1073 (2014).  
<https://doi.org/10.1134/S0036023614100076>
22. V. N. Fokin, E. E. Fokina, I. I. Korobov, et al., *Russ. J. Inorg. Chem.* **61**, 891 (2016).  
<https://doi.org/10.1134/S0036023616070044>
23. B. P. Tarasov, E. E. Fokina, and V. N. Fokin, *Russ. Chem. Bull.* **65**, 1887 (2016).  
<https://doi.org/10.1007/s11172-016-1529-2>

*Translated by O. Fedorova*